Journal of Magnetic Resonance **141,** 271–285 (1999)
Article ID jmre.1999.1885, available online at http://www.idealibrary.com on IDEAL®

Exact Product Operator Evolution of Weakly Coupled Spin-$\frac{1}{2}$ I_mS_n Systems during Arbitrary RF Irradiation of the I Spins

Thomas E. Skinner* and M. Robin Bendall†

**Physics Department, Wright State University, Dayton, Ohio 45435; and †Russell Grimwade School of Biochemistry and Molecular Biology, University of Melbourne, Parkville 3052, Victoria, Australia*

Received April 16, 1999; revised July 20, 1999

In this article, we consider the evolution of weakly coupled I_mS_n systems of spin-$\frac{1}{2}$ nuclei during arbitrary RF irradiation of the I spins. Exact solutions are presented for the time dependence of the density operator in terms of its constituent product operator components for a complete set of initial states derived from polarization of either the I or the S spin. The solutions extend the range of applications that are accessible to the product operator formalism and its associated vector picture of nuclear spin evolution. This marriage of quantum mechanics and a literal vector description of spin dynamics during RF irradiation supports physical intuition and has led to simple pulses for selective coherence transfer, among other new applications. The evolution of initial states that are free of transverse S-spin components can be described by classical precession of the I-spin components about effective fields defined by the interaction between the coupling and RF fields. Although there is no analogue involving classical rotations for the evolution of initial states composed of S_x or S_y, a vector description is still possible, and the solutions completely characterize the nature of J-coupling modulation during RF pulses. We emphasize the Cartesian product operator basis in the present treatment, but the solutions are readily obtained in any other basis that might prove suitable in analyzing an experiment. For a system of N coupled spins, standard exact methods involving diagonalization and multiplication of the $2^N \times 2^N$ matrices that represent the system require on the order of $(2^N)^3$ operations to calculate the system response to a general RF waveform at each point in the time domain. By contrast, the efficiency of the present method scales linearly with the number of spins. Since the formalism presented also accommodates the absence of either RF irradiation or the coupling, the solutions provide an efficient means of general pulse sequence simulation, encompassing any combination of arbitrary RF waveforms, delays, and coherence gradients.

Key Words: **product operators; radiofrequency; analytical solutions; spin systems; simulations.**

INTRODUCTION

The product operator formalism (*1, 2*) combines a rigorous quantum mechanical treatment of nuclear spin evolution with an intuitive physical picture to describe a broad class of NMR pulse sequences in which RF pulses act on a time scale that is short compared to time scales for *J*-coupling and chemical-shift evolution. A more complete picture which includes spin evolution during RF irradiation might be equally valuable for applications such as decoupling or selective pulses which currently fall outside the purview of this formalism. Recently, we proposed a vector model of decoupling that is applicable when the magnitude of the effective field seen by the irradiated spins is sufficiently greater than the coupling strength. The model accurately predicts the decoupled signal for any initial state of an IS system during a single ideal inversion pulse and is applicable to the analysis of different adiabatic decoupling schemes (*3*). However, in general, the effects of lower power RF pulses and phase cycling require a density matrix treatment that, while precise, provides little physical insight in its present form.

In this article, we derive the product operator transformations for a general I_mS_n system of weakly coupled, spin-$\frac{1}{2}$ heteronuclei during arbitrary RF irradiation of the I spins. Selective irradiation of a magnetically equivalent group of spins in a homonuclear experiment can thus be included in the formalism by assigning the label I to the selectively irradiated spins. The desired product operator form of the solutions arises naturally in the present work as a result of factoring the time-dependent density operator into products of the I-spin and S-spin angular momentum operators. The coefficients of individual product operator terms are simple linear combinations of the elements from $(n + 1)\ 2 \times 2$ matrices, so the calculations remain efficient even as the number of I and S spins in the system increases. No matrix diagonalization or multiplication of large matrices is required. These are computationally intensive procedures that would increase the number of operations in the calculations by about an order of magnitude for each spin added to the system.

We first consider the evolution of the S-spin magnetization and associated coherences, assumed, without loss of generality, to be on resonance. The basic formalism is then readily applied in a subsequent section to the evolution of the irradiated I-spin magnetization. Examples are provided that illustrate the simple patterns encoded in the formal solutions, together with recipes for constructing the solutions from a basic set of tabulated elements. The Discussion provides details on the computational efficiency

1090-7807/99 $30.00

of the results. Solutions are also considered for various limiting conditions of the applied RF field strength, followed by an analysis of the accuracy of solutions obtained using a popular approximation method. For constant RF, the solutions provide simple analytical expressions for the time dependence of the density operator as a function of its constituent product operator states that have revealed several new applications for weak RF fields (*4, 5*). Details of this and other work (*6*) that relied on the results presented here in full, sacrificed previously due to length constraints, are provided throughout the Discussion. We close by noting several applications for future work motivated by the vector picture that can be associated with the individual product operator states. We have found one reference in the literature that obtains a specific product operator solution for the evolution of the I spins in an IS system during RF of constant *x*-phase applied to I (*7*), but this work and its implications have apparently been overlooked.

EVOLUTION OF S-SPIN COHERENCE

The basic elements defining the I_mS_n problem considered here are contained in Waugh's analysis of the decoupled S-spin signal in an IS system (*8*), using matrix representations of the relevant operators. That work can be extended very simply to find the product operator components which comprise the density matrix: properly normalized, the trace of the density matrix times a given product operator state projects the density matrix onto that state. There are 16 product operator basis states in a spin-$\frac{1}{2}$ IS system, so this procedure is manageable for two spins. However, to avoid the cumbersome matrices that arise in larger spin systems, we employ standard spin-$\frac{1}{2}$ operator algebra. An example can be found in the comprehensive review of decoupling by Shaka and Keeler (*9*), which includes an expanded discussion of Waugh's calculation. These treatments deal exclusively with the observable signal from initial in-phase magnetization in an IS system. We consider a complete set of initial states for more general spin systems and calculate the evolution of the total density matrix in terms of its constituent product operator states. The procedure shows explicitly and simply which states are generated during the evolution of the density operator. The formalism is first outlined in some detail for an IS_n system, which provides the basis for the extensions which follow.

IS_n Systems

The Hamiltonian. In units of angular frequency, the effective RF field in the rotating frame of the I spins is

$$\boldsymbol{\omega}_e(t) = \omega_{rf}(t)[\cos\phi(t)\,\hat{\mathbf{x}} + \sin\phi(t)\,\hat{\mathbf{y}}] + \delta(t)\,\hat{\mathbf{z}}, \quad [1]$$

which encompasses any desired modulation of the amplitude (ω_{rf}), phase (ϕ), and frequency offset (δ), where offset is measured from the center of the I-spin sweep width. We follow the convention defined in (*1*) for right-hand rotations about any general $\boldsymbol{\omega} = -\gamma\mathbf{B}$, so that, for example, an on-resonance RF pulse applied along the $+x$ axis in the rotating frame produces, for positive γ, a right-hand rotation about $-x$. The RF phase ϕ is always the phase of $\boldsymbol{\omega}_{rf}$ in this convention, whereas the phase of the RF field depends on the sign of γ. The time-dependent Hamiltonian for an IS_n system can be written in the form

$$\mathcal{H}(t) = \boldsymbol{\omega}_e(t)\cdot\mathbf{I} + \mathcal{J}I_z\sum_{i=1}^{n} S_{iz}, \quad [2]$$

where $\mathcal{J}$ is 2π times the coupling, J, in Hertz, and S_{iz} is the z component of the ith S spin. Each operator is implicitly a direct product of the form $V^I \otimes V^{S_1} \otimes \ldots \otimes V^{S_n}$ for the $(n + 1)$ two-dimensional operators from each vector space of the individual I- and S-spin operators. Since operators from the different spaces commute, we will not necessarily maintain this particular ordering of the operators in what follows. The projection operators $P_i^{\pm}$ onto the spin-up (+) or spin-down (−) states in the S_i subspace are written in terms of S_{iz} and the identity operator, E_i, as

$$P_i^{\pm} = \tfrac{1}{2}E_i \pm S_{iz}, \quad [3]$$

so that

$$E_i = P_i^{+} + P_i^{-} \quad [4]$$

and

$$S_{iz} = 1/2(P_i^{+} - P_i^{-}). \quad [5]$$

In the vector space of an IS_3 system, for instance, we represent I_zS_{1z} as $\frac{1}{2}I_z(P_1^{+} - P_1^{-})E_2E_3$. Using this particular nomenclature for the projection or polarization operators instead of the commonly used alternative S_i^{α}, S_i^{β} provides a simple general algorithm for writing the Hamiltonian and time development operator and reduces the labor of calculation.

The Hamiltonian, recast in terms of these operators, is

$$\mathcal{H}(t) = \boldsymbol{\omega}_e(t)\cdot\mathbf{I}\prod_{i=1}^{n}(P_i^{+} + P_i^{-}) + \mathcal{J}/2\;I_z\sum_{i=1}^{n}(P_i^{+} - P_i^{-})\prod_{j\neq i}^{n}(P_j^{+} + P_j^{-}). \quad [6]$$

Performing the multiplications and grouping like terms yields a more concise expression. Define

$$\boldsymbol{\omega}_q(t) = \boldsymbol{\omega}_e(t) + q\mathcal{J}/2\;\hat{\mathbf{z}} \quad [7]$$

as the equivalent effective field seen by an uncoupled I-spin at a resonance offset $\delta + q\mathcal{J}/2$, oriented at an angle θ_q from the z axis given by

$$\tan\,\theta_q = \omega_{\rm rf}/[\delta + q\mathcal{J}/2]. \qquad [8]$$

Then, for example, with $n = 2$,

$$\begin{aligned}\mathcal{H}_{(n=2)} &= (\boldsymbol{\omega}_{\rm e}\cdot\mathbf{I} + 2\mathcal{J}/2\ I_z)\,P_1^+P_2^+ \\ &\quad + (\boldsymbol{\omega}_{\rm e}\cdot\mathbf{I} + 0\mathcal{J}/2\ I_z)(P_1^+P_2^- + P_1^-P_2^+) \\ &\quad + (\boldsymbol{\omega}_{\rm e}\cdot\mathbf{I} - 2\mathcal{J}/2\ I_z)\,P_1^-P_2^- \\ &= \boldsymbol{\omega}_{(+2)}\cdot\mathbf{I}\ P_1^+P_2^+ + \boldsymbol{\omega}_{(0)}\cdot\mathbf{I}\ (P_1^+P_2^- + P_1^-P_2^+) \\ &\quad + \boldsymbol{\omega}_{(-2)}\cdot\mathbf{I}\ P_1^-P_2^-. \end{aligned} \qquad [9]$$

More generally, for n spin-$\frac{1}{2}$ S operators, the maximum total S spin is $n/2$, with z components $n/2$, $(n/2 - 1)$, . . . , $-n/2$. For each product $P_1^{q_1}\ldots P_n^{q_n}$ that appears in $\mathcal{H}$, as illustrated above, the sum of the angular momenta $q_i = \pm 1$ (in units of half-integral spin) associated with the individual $P_i^{\pm}$ is

$$q_s = \sum_{i=1}^{n} q_i, \qquad [10]$$

which equals the coefficient of $\mathcal{J}/2$. We therefore write

$$\mathcal{H}(t) = \sum_{q_1,\ \ldots,\ q_n=\pm 1} \boldsymbol{\omega}_{q_s}(t)\cdot\mathbf{I}\prod_{j=1}^{n} P_j^{q_j}, \qquad [11]$$

which merely says that for an IS$_n$ system, the values of q_s range from $+n$ to $-n$, with $\Delta q_s = 2$. Each $\boldsymbol{\omega}_{q_s}\cdot\mathbf{I}$ is multiplied by all possible ways of generating a product of n different projection operators with total spin equal to q_s, for a total of 2^n terms, as illustrated previously for the $n = 2$ case in Eq. [9]. For $n = 3$, there are terms $\boldsymbol{\omega}_{\pm 3}\cdot\mathbf{I}\ P_1^{\pm}P_2^{\pm}P_3^{\pm}$ and three terms for $\boldsymbol{\omega}_{\pm 1}$ involving two $P^{\pm}$ and one $P^{\mp}$. The Hamiltonian for an IS system written in this form (*9*) consists of the two comparatively simple terms $\boldsymbol{\omega}_{\pm 1}\cdot\mathbf{I}\ P_1^{\pm}$. The basic constructs used in Eq. [11] and, hence, the simple algorithm described above, appear frequently as elements in the calculations which follow. Differences in the scalar couplings are readily incorporated by changing the component $q_s\mathcal{J}/2$ in each $\boldsymbol{\omega}_{q_s}$ defined by Eq. [7] to $\sum_{j=1}^{n} q_j\mathcal{J}_j/2$. Thus, $\boldsymbol{\omega}_{+1}$ in a term such as $\boldsymbol{\omega}_{+1}\cdot\mathbf{I}\ P_1^+P_2^-P_3^+$ would become $\boldsymbol{\omega}_{\rm e} + (\mathcal{J}_1 - \mathcal{J}_2 + \mathcal{J}_3)/2\ \hat{\mathbf{z}}$, for example.

The time evolution operator. The RF generated by the spectrometer is most commonly a digitized approximation of a continuous waveform in which the RF amplitude, phase, and frequency are constant during intervals of fixed length Δt. Thus, the Hamiltonian is time-independent at each time $t_k = k\Delta t$, and the exact expression for the time development operator or propagator $U(t_k,\ t_{k-1})$ between times t_{k-1} and t_k is simply $\exp[-i\mathcal{H}(t_k)\Delta t]$. In Eq. [11], the direct product of the n projection operators in each term sets one of the diagonal elements of the resulting $2^n \times 2^n$ projection operator equal to 1 and all other elements equal to zero. We define $\boldsymbol{\omega}_q^k = \boldsymbol{\omega}_q(t_k)$ and unit vector $\hat{\boldsymbol{\omega}}_q^k = \boldsymbol{\omega}_q^k/|\omega_q^k|$ with components determined by Eq. [7], together with a rotation angle

$$\beta_q^k = \tfrac{1}{2}\omega_q^k\Delta t. \qquad [12]$$

The propagator in matrix form is composed of the 2×2 elements

$$\begin{aligned} U_q(t_k,\ t_{k-1}) &= \exp[-i\boldsymbol{\omega}_q^k\cdot\mathbf{I}\ \Delta t] \\ &= \cos\,\beta_q^k - 2i(\hat{\boldsymbol{\omega}}_q^k\cdot\mathbf{I})\,\sin\,\beta_q^k \\ &= \begin{pmatrix} a_q^k & b_q^k \\ -b_q^{k*} & a_q^{k*}\end{pmatrix} \end{aligned} \qquad [13]$$

along the diagonal, where

$$\begin{aligned} a_q^k &= \cos\,\beta_q^k - i\hat{\omega}_{q,z}^k\,\sin\,\beta_q^k \\ b_q^k &= -(\hat{\omega}_{q,y}^k + i\hat{\omega}_{q,x}^k)\,\sin\,\beta_q^k \end{aligned} \qquad [14]$$

are the standard Cayley–Klein parameters for a rotation by $2\beta_q^k$ about $\hat{\boldsymbol{\omega}}_q^k$, and * represents complex conjugation. These parameters are utilized here primarily to simplify the notation and are not critical to the solutions. However, their connection to rotations is discussed briefly later (see Eq. [43]). For the $n = 2$ example, the diagonal elements are U_2, U_0, U_0, and U_{-2}, with multiplicities determined by the number of ways to combine n projection operators with total spin quantum number q. Starting at time t_0, the propagator to any later time t_k is obtained by successive application of the propagators for each of the k intervals, and the block-diagonal structure of U ensures that each block will also be a concatenation of the U_q, so that

$$U(t_k,\ t_0) = \sum_{q_1,\ \ldots,q_n=\pm 1} U_{q_s}(t_k,\ t_0)\prod_{j=1}^{n} P_j^{q_j}, \qquad [15]$$

similar to Eq. [11]. For a truly continuous RF waveform, this expression for the propagator would be an approximation that can be made increasingly accurate by decreasing the interval Δt. The C–K parameters $a_q(t_k,\ t_0)$ and $b_q(t_k,\ t_0)$, which describe an evolution from an initial time t_0 to a final time t_k, are obtained by the recurrence relation given in the Appendix, which uses half the operations required by the full 2×2 matrix multiplications involved in concatenating $U_q(t_k,\ t_{k-1})$ at successive time intervals (see also Ref. (*10*)). The k sets of C–K parameters and, hence, the time evolution of the system, are

therefore predetermined by the RF waveform at the start of the experiment. We will use the abbreviated notation a_q and b_q to describe either the incremental form $U_q(t_k, t_{k-1})$ or the total effective propagator $U_q(t_k, t_0)$ in the subspace labeled by q when the distinction is clear from the context in which they are used.

The density operator. The state of the system at time t is embodied in the density operator, which evolves from an initial state $\rho(t_0)$ according to the relation

$$\rho(t) = U(t, t_0)\rho(t_0)U^\dagger(t, t_0). \quad [16]$$

We consider the set of four initial conditions

$$\rho_\nu(t_0) \in \{S_x, 2S_yI_x, 2S_yI_y, 2S_yI_z\} \quad (\nu = 0, 1, 2, 3), \quad [17]$$

composed of transverse S-spin operators and assign the label ν sequentially to members of the set. We write the x_j component of the I spin as I_{x_j} for $(x_1, x_2, x_3) \doteq (x, y, z)$ and define $I_{x_0} = \frac{1}{2}E$, giving $\rho_0(t_0) = 2S_xI_{x_0}$ to complete the symmetry of the set. As will be shown in the next section, the set is closed for an IS system in the sense that there is no evolution to any state that is not a member of the set. Each S-spin operator is a sum $\sum_{j=1}^{n} S_j$, which is implicit in the notation. We also employ the usual raising and lowering operators

$$S_j^\pm = S_{jx} \pm iS_{jy}, \quad [18]$$

which can be obtained by interchanging the two columns of $P_j^\pm$ in the matrix representation.

In the calculation of $\rho_\nu(t)$, the product $U\rho_\nu(t_0)$ produces terms $P_j^\pm S_{jx} = (\frac{1}{2})S_j^\pm$ and $P_j^\pm S_{jy} = \mp(i/2)S_j^\pm$. The operators $(P_j^\pm)^\dagger$ in the adjoint operator $U^\dagger$ are equal to $P_j^\pm$, giving terms $P_j^\pm P_j^\mp = 0$, $S_j^\pm P_j^\pm = 0$, and $S_j^\pm P_j^\mp = S_j^\pm$. Thus, the only nonzero terms in Eq. [16] are those containing factors of the form $P_j^\pm S_{jx} P_j^\mp = (\frac{1}{2})S_j^\pm$ and $P_j^\pm S_{jy} P_j^\mp = \mp(i/2)S_j^\pm$. This reduces the density operator to an expression analogous to Eq. [9], with the product of projection operators in each term replaced by the sum of unique products in which a single $P_j^\pm$ is converted to $S_j^\pm$. As an example using the initial condition $\nu = 2$ for the IS_2 case,

$$\begin{aligned} U &= P_1^+P_2^+U_{(+2)} + (P_1^+P_2^- + P_1^-P_2^+)U_{(0)} \\ &\quad + P_1^-P_2^-U_{(-2)} \\ \rho_2(t_0) &= 2I_y(S_{1y} + S_{2y}) \\ U^\dagger &= P_1^+P_2^+U_{(+2)}^\dagger + (P_1^+P_2^- + P_1^-P_2^+)U_{(0)}^\dagger \\ &\quad + P_1^-P_2^-U_{(-2)}^\dagger. \end{aligned} \quad [19]$$

Picking out the nonzero terms from the product $U\rho_2(t_0)U^\dagger$ and using the relation $S^- = (S^+)^\dagger$ results in terms of the form

$$\begin{aligned} Z &= (S_1^+P_2^+ + P_1^+S_2^+)U_{(+2)}2I_yU_{(0)}^\dagger \\ &\quad + (S_1^+P_2^- + P_1^-S_2^+)U_{(0)}2I_yU_{(-2)}^\dagger, \end{aligned} \quad [20]$$

to give

$$\begin{aligned} \rho_2(t) &= -i/2[Z - Z^\dagger] \\ &= \mathrm{Im}[Z]. \end{aligned} \quad [21]$$

For the other initial conditions, the I-spin operator becomes I_{x_ν} in the expression for Z. In addition, for initial S_x ($\nu = 0$), the terms $P_j^\pm S_{jx} P_j^\mp = (\frac{1}{2})S_j^\pm$ that arise in the calculation of $\rho_0(t)$ give only positive coefficients to produce terms of the form $Z + Z^\dagger$, resulting in the real part of Z instead of the imaginary part.

Therefore, for general n, the simple algorithm that generates the equation for $\rho_\nu(t)$ is (i) construct the terms $U_{(q)}2I_{x_\nu}U_{(q-2)}^\dagger$ for $q = n, n-2, \ldots, -(n-2)$ and then (ii) multiply each term by all combinations of a single S_i^+ ($i = 1, \ldots, n$) and $n-1$ operators $P_j^\pm$ ($j \neq i$) with total angular momentum equal to q. This procedure is described more formally by the expression

$$Z_\nu(t) = \sum_{i=1}^{n} \sum_{\substack{q_1, \ldots, q_n = \pm 1 \\ q_i \neq -1}} [U_{(q_s)}2I_{x_\nu}U_{(q_s-2)}^\dagger][S_i^{q_i} \prod_{j \neq i}^{n} P_j^{q_j}], \quad [22]$$

giving

$$\rho_\nu(t) = \begin{cases} \mathrm{Re}[Z_\nu] & \nu = 0 \quad (\text{initial in-phase } S_x) \\ \mathrm{Im}[Z_\nu] & \nu \neq 0 \quad (\text{initial } 2S_yI_{x_\nu} \text{ coherence}). \end{cases} \quad [23]$$

The bracketed expressions in Eq. [22] provide, in turn, the I-spin and S-spin constituents of $\rho_\nu(t)$.

The solution for the density operator can thus be reduced to calculating the general products $U_q2I_{x_\nu}U_r^\dagger$. Using Eq. [13] for the effective propagator in each subspace, these can be expanded as linear combinations of the Pauli basis set, $2I_{x_\mu}$, as

$$U_q2I_{x_\nu}U_r^\dagger = \sum_{\mu=0}^{3} \alpha_{\nu\mu}^{(q,r)}2I_{x_\mu} \quad [24]$$

to obtain the simple expressions for the expansion coefficients $[\alpha]_\mu$ listed in Table 1 as a function of the indices ν, q, and r. Table 2 translates these coefficients to their expressions in terms of the C–K parameters in Eqs. [14] and [A3]. Details are provided in the Appendix. Although each U_q is a rotation operator, we note that the transformation of each component I_{x_j} of the quantum-mechanical vector operator $\mathbf{I}$ in Eq. [24] is a classical rotation only for $q = r$. By contrast, the transformation of the identity element $U_{(q)}2I_{x_0}U_{(q-2)}^\dagger = U_{(q)}U_{(q-2)}^\dagger$ that

TABLE 1

μ / ν	0 ($2I_{x_0}$)	1 ($2I_x$)	2 ($2I_y$)	3 ($2I_z$)
0	$\mathrm{Re}[A_0^{(q,r)}]$	$i\ \mathrm{Im}[B_0^{(q,r)}]$	$i\ \mathrm{Re}[B_0^{(q,r)}]$	$i\ \mathrm{Im}[A_0^{(q,r)}]$
1	$i\ \mathrm{Im}[A_1^{(q,r)}]$	$\mathrm{Re}[B_1^{(q,r)}]$	$-\mathrm{Im}[B_1^{(q,r)}]$	$\mathrm{Re}[A_1^{(q,r)}]$
2	$-i\ \mathrm{Re}[A_2^{(q,r)}]$	$\mathrm{Im}[B_2^{(q,r)}]$	$\mathrm{Re}[B_2^{(q,r)}]$	$\mathrm{Im}[A_2^{(q,r)}]$
3	$i\ \mathrm{Im}[A_3^{(q,r)}]$	$\mathrm{Re}[B_3^{(q,r)}]$	$-\mathrm{Im}[B_3^{(q,r)}]$	$\mathrm{Re}[A_3^{(q,r)}]$

Note. Coefficients $\alpha_{\nu\mu}^{(q,r)}$ of the Pauli matrices $2I_{x_\mu}$, with $2I_{x_0}$ equal to the identity operator, are tabulated for the expansion of the product $U_q 2I_{x_\nu} U_r^\dagger$ in Eq. [24] given the initial conditions denoted by ν in Eq. [17]. The expansion coefficients are written in terms of $A_\nu^{(q,r)}$ and $B_\nu^{(q,r)}$ defined in Table 2. Details of the derivation are provided in the Appendix. For applications in the text, $r = q - 2$.

TABLE 2

ν	$A_\nu^{(q,r)}$	$B_\nu^{(q,r)}$
0	$a_q a_r^* + b_q b_r^*$	$-a_q b_r + b_q a_r$
1	$a_q b_r^* + b_q a_r^*$	$a_q a_r - b_q b_r$
2	$a_q b_r^* - b_q a_r^*$	$a_q a_r + b_q b_r$
3	$a_q a_r^* - b_q b_r^*$	$-a_q b_r - b_q a_r$

Note. The elements $A_\nu^{(q,r)}$ and $B_\nu^{(q,r)}$ of Table 1 are listed as functions of the Cayley–Klein parameters defined in Eq. [14] and Eq. [A3], as outlined in the discussion leading to Eq. [A5] in the Appendix. Complex conjugation is denoted by *.

arises in the calculation of $\rho_0(t)$ starting with initial in-phase S_x is decidedly nonclassical, generating I-spin components where there were previously none.

The solution for the density operator is completed using Eq. [18] for S_i^+ and Eq. [3] for $P_j^\pm$ to perform the multiplications in Eq. [22], keeping only the real terms for initial in-phase magnetization or the imaginary terms for coherences $2S_y I_{x_j}$ at the start of the RF irradiation. As an illustration, we consider the solution $\rho_\nu(t)$ that evolves when RF is applied to the I spins in an IS_3 system that is initially in the $\nu = 0$ state, $\rho_0(t_0) = S_x$. According to Eq. [23], $\rho_0(t) = \mathrm{Re}[Z_0]$, and Z_0 is easily constructed by analogy to the IS_2 example given in Eq. [20] for $\nu = 2$ (see, for example, the text preceding Eq. [22], which formally defines the algorithm). The elements $\alpha_{0\mu}$ for general (q, r) listed in row $\nu = 0$ of Table 1 determine the components I_{x_μ} in Z_0. Since α_{00} is real, only terms involving S_{ix} and S_{jz}, from the products $S_i^+ P_j^\pm$, are associated with $2I_{x_0} = E$. Since the α_{0j} $(j = 1, 2, 3)$ are imaginary, $\mathrm{Re}[Z_0]$ associates similar terms involving S_{iy} and S_{jz} with $2I_{x_j}$. In the interest of brevity, we write out fully only the terms involving S_{ix} to obtain

$$\begin{aligned}\rho_0(t) \propto\ & \mathrm{Re}[A_0^{(3,1)} + 2A_0^{(1,-1)} + A_0^{(-1,-3)}] \sum_{i=1}^{n} (S_i)_x \\ & + \mathrm{Re}[A_0^{(3,1)} - A_0^{(-1,-3)}]\ 2\ [S_{1x}(S_{2z} + S_{3z}) \\ & \quad + S_{2x}(S_{1z} + S_{3z}) + S_{3x}(S_{1z} + S_{2z})] \\ & + \mathrm{Re}[A_0^{(3,1)} - 2A_0^{(1,-1)} + A_0^{(-1,-3)}] \\ & \times 4[S_{1x}S_{2z}S_{3z} + S_{2x}S_{1z}S_{3z} + S_{3x}S_{1z}S_{2z}] \\ & + \{2S_y I_{x_j} + \ldots \text{terms}\}.\end{aligned} \qquad [25]$$

Coefficients of the $2S_y I_{x_j}$ terms have the same functional form shown above for the S_x terms, but are constructed from the other elements in row $\nu = 0$ of Table 1.

Thus, there are n levels of product operator terms for an IS_n system, depending on the number of S-spin operators in the product. The functions $f_i^n(\Omega)$ listed in row i, column n of Table 3 multiply terms consisting of products of i S-spin operators, with $i \leq n$. The f_i^n with $i > n$ are zero, so the solutions for $\rho_\nu(t)$ become progressively simpler for smaller n. For an IS_2 system, terms involving S_{3x} and S_{3z} are eliminated, and the coefficients change to the form given in column 2 of Table 3. For an IS system, there are no terms involving S_{2x} and S_{2z}, and the coefficients change to the form given in column 1 of Table 3. The particular arguments $\Omega_{\nu\mu}$ of the functions depend on the initial condition, denoted by ν, and on the component $2I_{x_\mu}$ in the product. They are listed in Table 4 for general (q, r) in terms of A_ν and B_ν tabulated earlier in Table 2. For example, the terms involving operator $2SyI_x$ in Eq. [25] $(n = 3)$ require Ω_{01} of Table 4 and the three functions f_i^3 of $\Omega_{01} = \mathrm{Im}[B_0]$ in column 3 of Table 3. We merely take the terms involving $2I_{x_0}$ which are written out fully as functions of $\Omega_{00}^{(q,r)} = \mathrm{Re}[A_0^{(q,r)}]$ and change I_{x_0} to I_x, S_x to S_y, and $\mathrm{Re}[A_0]$ to $-\mathrm{Im}[B_0]$. The remaining terms are generated similarly using the other elements in row zero of Table 4. Solutions for the evolution of initial states labeled by index ν in Eq. [17] are constructed similarly using row ν of Table 4.

TABLE 3

i	IS	IS_2	IS_3
1	$\Omega^{(1,-1)}$	$\Omega^{(2,0)} + \Omega^{(0,-2)}$	$\Omega^{(3,1)} + 2\Omega^{(1,-1)} + \Omega^{(-1,-3)}$
2	0	$\Omega^{(2,0)} - \Omega^{(0,-2)}$	$\Omega^{(3,1)} - \Omega^{(-1,-3)}$
3	0	0	$\Omega^{(3,1)} - 2\Omega^{(1,-1)} + \Omega^{(-1,-3)}$

Note. Solutions for the density operator $\rho_\nu(t)$ during irradiation of the I spins in an $I_m S_n$ system are provided in Eq. [26] $(m = 1)$ and Eq. [38] $(m > 1)$ for the initial states denoted by ν in Eq. [17], which are derived from the S-spin polarization. The product operator coefficients $f_i^n(\Omega)$ in the solution are tabulated in column n. The subscript i denotes the number of S-spin operators in a product. For $m = 1$, Table 4 lists the specific arguments $\Omega_{\nu\mu}$, corresponding to terms containing I_{x_μ} in the solution for $\rho_\nu(t)$. An example illustrating the application of Table 3 to Eq. [26] for the specific case of an IS_3 system starting with the initial state S_x $(\nu = 0)$ is provided in Eq. [25] and the discussion thereafter. Solutions for the other initial conditions are obtained by substituting the elements in row ν of Table 4 for those elements shown in Eq. [25]. The solutions become progressively simpler for smaller n, since $f_i^n = 0$ for $i > n$. Arguments to f_i^n for general m in Eq. [38] are given in Eqs. [34] and [36].

TABLE 4

μ / ν	0 (S_x)	1 ($2S_yI_x$)	2 ($2S_yI_y$)	3 ($2S_yI_z$)
0	$\mathrm{Re}[A_0^{(q,r)}]$	$-\mathrm{Im}[B_0^{(q,r)}]$	$-\mathrm{Re}[B_0^{(q,r)}]$	$-\mathrm{Im}[A_0^{(q,r)}]$
1	$\mathrm{Im}[A_1^{(q,r)}]$	$\mathrm{Re}[B_1^{(q,r)}]$	$-\mathrm{Im}[B_1^{(q,r)}]$	$\mathrm{Re}[A_1^{(q,r)}]$
2	$-\mathrm{Re}[A_2^{(q,r)}]$	$\mathrm{Im}[B_2^{(q,r)}]$	$\mathrm{Re}[B_2^{(q,r)}]$	$\mathrm{Im}[A_2^{(q,r)}]$
3	$\mathrm{Im}[A_3^{(q,r)}]$	$\mathrm{Re}[B_3^{(q,r)}]$	$-\mathrm{Im}[B_3^{(q,r)}]$	$\mathrm{Re}[A_3^{(q,r)}]$

Note. The elements $\Omega_{\nu\mu}^{(q,r)}$ of Table 3 ($r = q - 2$) that appear in the Eq. [26] solution for the density operator $\rho_\nu(t)$ in an IS_n system starting with the initial condition denoted by ν in Eq. [17] are listed as functions of $A_\nu^{(q,r)}$ and $B_\nu^{(q,r)}$ defined in Table 2. For a simple IS system, $\Omega_{\nu\mu}^{(1,-1)}$ is the coefficient of the product operator displayed in the heading for column μ. For general IS_n, the coefficients of these same operators are given by the linear combinations in row 1 of Table 3, with coefficients of the additional product operators that arise for $n > 1$ listed in rows 2 and 3, as illustrated for an IS_3 system in Eq. [25].

The final result for general n and initial condition ν can be written succinctly as

$$\rho_\nu(t) = \frac{1}{2^{n-1}} \sum_{i=1}^{n} \Bigg(S_{i,x} \Big\{ f_1^n(\Omega_{\nu 0}) + 2 \sum_{j\neq i}^{n} S_{j,z} [\, f_2^n(\Omega_{\nu 0}) + 2 \sum_{\substack{k>j \\ k\neq i}}^{n} S_{k,z} f_3^n(\Omega_{\nu 0})] \Big\} + 2 \sum_{r=1}^{3} I_{x_r} S_{i,y} \Big\{ f_1^n(\Omega_{\nu r}) + 2 \sum_{j\neq i}^{n} S_{j,z} [\, f_2^n(\Omega_{\nu r}) + 2 \sum_{\substack{k>j \\ k\neq i}}^{n} S_{k,z} f_3^n(\Omega_{\nu r})] \Big\} \Bigg). \quad [26]$$

As an example, Eq. [25] was provided to show the explicit correspondence between terms involving $S_{i,x}$ in Eq. [26] for an IS_3 system starting with initial S_x ($\nu = 0$).

The observed signal, $\langle S_x(t) \rangle \propto \mathrm{Tr}[S_x \rho_\nu(t)]$, is proportional to $f_1^n(\Omega_{\nu 0})$, since only the S_x^2 terms have nonzero trace. The other terms give the relative proportions of the different coherences that have evolved. Alternatively, the expansion in Eq. [24] can be performed just as readily in terms of either $I^\pm$ or the related spherical tensor basis if these forms of the solution are required, or the desired transformations between bases can be performed on the final result.

I_mS_n Systems

The previous results can easily be extended to obtain the solutions for an $\mathrm{I}_m\mathrm{S}_n$ system. We write the x_j component of the ith I spin as I_{i,x_j}. For the ith I spin, Eq. [11] becomes

$$\mathcal{H}_i(t) = - \sum_{q_1,\ldots,q_n=\pm 1} \boldsymbol{\omega}_{q_s} \cdot \mathbf{I}_i \prod_{j=1}^{n} P_j^{q_j}, \quad [27]$$

so that $\mathcal{H}(t) = \sum_{i=1}^{m} \mathcal{H}_i$. Although the Hamiltonian no longer exhibits the simple 2×2 block-diagonal structure of the IS_n systems, the individual $\mathcal{H}_i$ commute among themselves. In addition, all the terms in $\mathcal{H}_i$ commute, since each term contains a unique product of projection operators, which guarantees that the commutator has at least one product of the form $P_j^\pm P_j^\mp = 0$ for each term. The propagator is still written as in Eq. [15], but now

$$U_{(q_s)}(t_k, t_0) = \prod_{i=1}^{m} U_{i\,(q_s)}(t_k, t_0). \quad [28]$$

The evolution of the density operator, described in Eqs. [16] through [23], follows immediately, with a minor modification to Eq. [22] for Z_ν. Define the function $\Upsilon(m, q)$ as the product

$$\Upsilon(m, q) = \prod_{k=1}^{m} U_{k(q)} U_{k(q-2)}^\dagger \quad [29]$$

and define

$$\Upsilon(m, x_j, q) = \sum_{k=1}^{m} (U_{k(q)} 2I_{k,x_j} U_{k(q-2)}^\dagger \prod_{l\neq k}^{m} U_{l(q)} U_{l(q-2)}^\dagger). \quad [30]$$

Then

$$Z_\nu(t) \rightarrow \begin{cases} \displaystyle\sum_{i=1}^{n} \sum_{\substack{q_1,\ldots,q_n=\pm 1 \\ q_i\neq -1}} \Upsilon(m, q_s)\, S_i^{q_i} \prod_{j\neq i}^{n} P_j^{q_j} & \nu = 0 \\ \displaystyle\sum_{i=1}^{n} \sum_{\substack{q_1,\ldots,q_n=\pm 1 \\ q_i\neq -1}} \Upsilon(m, x_j, q_s)\, S_i^{q_i} \prod_{j\neq i}^{n} P_j^{q_j} & \nu \neq 0 \end{cases} \quad [31]$$

and the final solution for the density operator is still given by Eq. [23].

Single S-spin. For in-phase S_x at the start of the I-spin irradiation, $\rho_0(t)$ is obtained from Z_0 in Eq. [31] as

$$\rho_0(t) = \mathrm{Re}[S^+ \Upsilon(m, +1)] = \mathrm{Re}[(S_x + iS_y)\Upsilon(m, +1)]. \quad [32]$$

According to Eq. [24] defining the general matrix $\alpha_{\nu\mu}^{(q,r)}$ listed in Table 1, $\Upsilon(m, q)$ is all possible products of m elements from row zero, so that, most generally,

$$\Upsilon(m, q) = 2^m \sum_{\mu_1, \ldots, \mu_m=0}^{3} [\alpha_{0\mu_1}^{(q,q-2)} \ldots \alpha_{0\mu_m}^{(q,q-2)}][I_{\mu_1} \ldots I_{\mu_m}], \quad [33]$$

where α_{00} is pure real and α_{0j} ($j = 1, 2, 3$) is pure imaginary.

The terms multiplying S_x in Eq. [32] for $\rho_0(t)$ must be the real part of $\Upsilon(m, +1)$, so the coefficient of $S_x = 2S_xI_{x_0}$ is immediately seen to be $(\alpha_{00}^{1,-1})^m = [\mathrm{Re}(A_0^{1,-1})]^m$. Operators of the form $4S_xI_{x_j}I_{x_k}$ result from multiplying two imaginary elements from columns 1 through 3 for an I_2S system and using $2I_{x_0}$ for the required third real element in an I_3S system. Terms multiplying iS_y must be pure imaginary to produce a real result, leading to operators of the form $2S_yI_{x_j}$ and, for I_3S, additional operators $8S_xI_{x_j}I_{x_k}I_{x_l}$. The $m = 1$ result for an IS system is given in Eq. [26] as functions of the pure real elements $\Omega_{\nu\mu}$ in Table 4, where $\alpha_{0j} = -i\Omega_{0j}$ and $\alpha_{j0} = i\Omega_{j0}$ ($j = 1, 2, 3$). More generally, we can select the terms from Eq. [33] that satisfy the above requirements to define the resulting coefficients of the S_x and S_y operators in terms of general indices (q, r) as

$$c_{0,x}^{(q,r)} = [\Omega_{00}^{(q,r)}]^m - \frac{m-1}{2^{m-2}} 4\,[\Omega_{00}^{(q,r)}]^{m-2} \times \sum_{k,l=1}^{3} \Omega_{0k}^{(q,r)}\Omega_{0l}^{(q,r)} \Big(\sum_{p=1}^{m-1}\sum_{s>p}^{m} I_{p,x_k}I_{s,x_l}\Big)$$

$$c_{0,y}^{(q,r)} = 2[(\Omega_{00}^{(q,r)}]^{m-1} \sum_{k=1}^{3} \Omega_{0k}^{(q,r)} I_{x_k} - \tfrac{1}{2}(m-1)(m-2) \times 8 \sum_{k,l,p=1}^{3} \Omega_{0k}^{(q,r)}\Omega_{0l}^{(q,r)}\Omega_{0p}^{(q,r)} I_{1,x_k}I_{2,x_l}I_{3,x_p} \quad [34]$$

for $m = 1, 2, 3$.

The density operator resulting from the initial state $2S_yI_{x_j}$, with $I_{x_j} = \sum_{i=1}^{m} I_{i,x_j}$, is obtained from Z_j in Eq. [31] as

$$\rho_j(t) = \mathrm{Im}[S^+\Upsilon(m, x_j, +1)]. \quad [35]$$

From Eq. [30] defining $\Upsilon(m, x_j, q)$, there is a factor $U_{(+1)}2I_{i,x_j}U_{(-1)}^\dagger$ given by row j of Table 1 for a single I spin, multiplied by $U_{(+1)}U_{(-1)}^\dagger$ for the remaining $m - 1$ spins. This process is repeated for each I spin contained in the sum over the individual spins, and the final result must be imaginary. Compared to row zero of Table 1, the elements which are either pure real or pure imaginary in rows 1–3 are interchanged, so the solutions for $\rho_j(t)$ can be taken from the $\rho_0(t)$ results by adding all combinations in Eq. [34] that replace a single element from row zero with one from row j. The coefficients of the S_x and S_y operators can then be written in general form for this case as

$$c_{j,x}^{(q,r)} = m\Omega_{j0}^{(q,r)}(\Omega_{00}^{(q,r)})^{m-1} - \frac{m-1}{2^{m-2}} \times 4 \sum_{k,l=1}^{3} [(m-2)\Omega_{j0}^{(q,r)}\Omega_{0k}^{(q,r)}\Omega_{0l}^{(q,r)} + (\Omega_{00}^{(q,r)})^{m-2}(\Omega_{jk}^{(q,r)}\Omega_{0l}^{(q,r)} + \Omega_{0k}^{(q,r)}\Omega_{jl}^{(q,r)})] \times [\sum_{p=1}^{m-1}\sum_{s>p}^{m} I_{p,x_k}I_{s,x_l}]$$

$$c_{j,y}^{(q,r)} = 2\sum_{k=1}^{3} [(\Omega_{00}^{(q,r)})^{m-1}\Omega_{jk}^{(q,r)} + (m-1) \times (\Omega_{00}^{(q,r)})^{m-2}\Omega_{j0}^{(q,r)}\Omega_{0k}^{(q,r)}]I_{x_k} - \tfrac{1}{2}(m-1)(m-2)\, 8 \sum_{k,l,p=1}^{3} (\Omega_{jk}^{(q,r)}\Omega_{0l}^{(q,r)}\Omega_{0p}^{(q,r)} + \Omega_{0k}^{(q,r)}\Omega_{jl}^{(q,r)}\Omega_{0p}^{(q,r)} + \Omega_{0k}^{(q,r)}\Omega_{0l}^{(q,r)}\Omega_{jp}^{(q,r)})I_{1,x_k}I_{2,x_l}I_{3,x_p}, \quad [36]$$

so that, combining these results,

$$\rho_\nu(t) = c_{\nu,x}^{(1,-1)}S_x + c_{\nu,y}^{(1,-1)}S_y \quad [37]$$

for an I_mS system starting with the initial conditions denoted by $\nu = 0, \ldots, 3$ of Eq. [17]. The expressions given in Eqs. [34] and [36] for the coefficients show explicitly which I-spin operators contribute as the number, m, of I spins increases.

Multiple S-spins. For $n > 1$, terms of the form $S_i\Pi_jP_j$ in Eq. [31] result in the same products of S-spin operators as for the IS_n case. Noting that the terms involving components of the total I-spin operator for m I spins are included in the expressions for $c_{\nu,x}$ and $c_{\nu,y}$ derived above, we can immediately write from Eq. [26]

$$\rho_\nu(t) = \frac{1}{2^{n-1}} \sum_{i=1}^{n} \Bigg(S_{i,x}\Big\{f_1^n(c_{\nu,x}) + 2\sum_{j\neq i}^{n} S_{j,z}[\,f_2^n(c_{\nu,x}) + 2\sum_{\substack{k>j\\k\neq i}}^{n} S_{k,z}f_3^n(c_{\nu,x})]\Big\} + 2S_{i,y}\Big\{f_1^n(c_{\nu,y}) + 2\sum_{j\neq i}^{n} S_{j,z}[\,f_2^n(c_{\nu,y}) + 2\sum_{\substack{k>j\\k\neq i}}^{n} S_{k,z}f_3^n(c_{\nu,y})]\Big\}\Bigg), \quad [38]$$

using the functions f_i^n from Table 3. Although the proliferation of products operator terms becomes somewhat unwieldy as the num-

TABLE 5

$$\begin{pmatrix} \cos^2\phi(\sin^2\theta_q + \cos^2\theta_q\cos 2\beta_q) + \sin^2\phi\cos 2\beta_q & \sin 2\phi\sin^2\theta_q\sin^2\beta_q - \cos\theta_q\sin 2\beta_q & \cos\phi\sin 2\theta_q\sin^2\beta_q + \sin\phi\sin\theta_q\sin 2\beta_q \\ \sin 2\phi\sin^2\theta_q\sin^2\beta_q + \cos\theta_q\sin 2\beta_q & \sin^2\phi(\sin^2\theta_q + \cos^2\theta_q\cos 2\beta_q) + \cos^2\phi\cos 2\beta_q & \sin\phi\sin 2\theta_q\sin^2\beta_q - \cos\phi\sin\theta_q\sin 2\beta_q \\ \cos\phi\sin 2\theta_q\sin^2\beta_q - \sin\phi\sin\theta_q\sin 2\beta_q & \sin\phi\sin 2\theta_q\sin^2\beta_q + \cos\phi\sin\theta_q\sin 2\beta_q & \cos^2\theta_q + \sin^2\theta_q\cos 2\beta_q \end{pmatrix}$$

Note. The matrix $\boldsymbol{R}_q$ produces a classical rotation of a vector by angle $2\beta_q$ about an axis oriented at a polar angle θ_q from the z axis and azimuthal axis ϕ from the x axis in the transverse plane. The equivalent effective field $\boldsymbol{\omega}_q$ arising from the interaction between the coupling and the RF fields, as given in Eq. [7], completely determines the rotation parameters through the relations defined in Eqs. [1], [8], and [12].

ber of I and S spins increases, the observable magnetization S_x and coherences $2S_yI_{x_j}$ are readily extracted by inspection. In addition, this expression is straightforward to program for simulations. Variations in the scalar couplings are handled as for the IS_n case, with an additional modification of $\boldsymbol{\omega}_{q_s}$ for each I spin, leading to separate versions of Table 4 labeled by the I spin and corresponding modifications of Eqs. [34] and [36].

EVOLUTION OF I-SPIN COHERENCE

This section provides solutions for the evolution of the I-spin magnetization and associated coherences involving only longitudinal S_z that were not considered in the previous section. The formalism shows immediately that these can be viewed as classical rotations about effective fields that incorporate the coupling, which allows the solutions to be written down by inspection.

IS_n Systems

The propagator is still given by Eq. [15], and we consider the set of six initial states

$$\rho(t_0) \in \{I_{x_j},\ 2I_{x_j}S_z\}. \qquad [39]$$

As for the initial conditions listed in Eq. [17] of the previous section, the members of this set only evolve, for an IS system, to members within the set. The time development of the system is given by

$$\rho(t) = U(t,\ t_0)\rho(t_0)U^\dagger(t,\ t_0)$$

$$= \sum_{q_1,\ \ldots\ ,q_n=\pm 1} U_{q_s}\,\rho(t_0)U_{q_s}^\dagger \prod_{j=1}^{n} P_k^{q_j}, \qquad [40]$$

which follows from $P_k^{\pm}P_k^{\mp} = 0$ and $2P_k^{\pm}S_z = \pm P_k^{\pm}$. The sums and products that appear in Eq. [40] are parsed in the discussion surrounding Eq. [11]. Thus, the solution for the density operator again reduces to calculating products of the form $U_qI_{x_j}U_r^\dagger$, similar to Eq. [22], and we could proceed with the expansion in terms of the Pauli basis as in the previous section. However, Eq. [22] was obtained for initial states involving transverse S-spin operators, which, in turn, forced $r = q - 2$. This mixing of propagators associated with different allowed values for the magnetic quantum number of the total S-spin angular momentum has no classical analogue, as noted earlier. In the present case, where $r = q$, each term of the form $U_qI_{x_j}U_q^\dagger$ in Eq. [40] can be immediately recognized as the transformation that generates a classical rotation of each component of the quantum-mechanical vector operator **I** about $\boldsymbol{\omega}_q$, and the solutions can be obtained by inspection using standard matrix results for a 3D rotation about an arbitrary axis. The desired rotation matrix $\boldsymbol{R}_q$ is listed in Table 5 in terms of the RF phase angle ϕ, the polar angle θ_q given in Eq. [8], and rotation angle β_q of Eq. [12]. The rotated I-spin components are then multiplied by the specified products of the projection operators $P_k^{\pm} = \frac{1}{2}E_k \pm S_{kz}$.

For $n = 1$, there are product operator terms involving both no S spins and a single S_z, so that

$$2I_{x_j} \rightarrow [\boldsymbol{R}_{(+1)} + \boldsymbol{R}_{(-1)}]I_{x_j} + [\boldsymbol{R}_{(+1)} - \boldsymbol{R}_{(-1)}]2I_{x_j}S_z \quad (n = 1), \qquad [41]$$

where the rotations $\boldsymbol{R}_{(\pm 1)}$ act only on the I-spin operator. An RF phase $\phi = 0$ reproduces the solution in Ref. (*7*). For $n = 2$, there are rotations $\{\boldsymbol{R}_{(\pm 2)},\ \boldsymbol{R}_{(0)}\}$ and an additional product $S_{1z}S_{2z}$, which, for $n = 3$, expands to include $S_{1z}S_{3z}$ and $S_{2z}S_{3z}$ plus a term involving three S spins, $S_{1z}S_{2z}S_{3z}$, together with rotations $\{\boldsymbol{R}_{(\pm 3)}, \boldsymbol{R}_{(\pm 1)}\}$ acting on the given I-spin operator. The functions $g_\nu^n(\boldsymbol{R})$ of the specific rotation matrices which give the coefficients of these operators are tabulated in Table 6, where (as for the functions f_i^n in Table 3) the superscript n is the number of S spins in the system and the subscript $\nu = 0, \ldots, n$ gives the number of S spins in the particular product operator term. The results, again, are of similar structure to Eq. [26], and we obtain, for $\rho_j(t_0) = I_{x_j}$,

$$\rho_j(t) = \frac{1}{2^n}\left(g_0^n(\boldsymbol{R}) + 2\sum_{i=1}^{n} S_{i,z}\Big\{ g_1^n(\boldsymbol{R}) + 2\sum_{k>i}^{n} S_{k,z}\big[\, g_2^n(\boldsymbol{R}) + 2\sum_{l>k}^{n} S_{l,z}g_3^n(\boldsymbol{R})\big]\Big\}\right) I_{x_j}. \qquad [42]$$

This equation can be used for the initial state $2I_{x_j}S_z$ by multi-

TABLE 6

ν	IS	IS_2	IS_3
1	$\boldsymbol{R}_{(+1)} + \boldsymbol{R}_{(-1)}$	$\boldsymbol{R}_{(+2)} + 2\boldsymbol{R}_{(0)} + \boldsymbol{R}_{(-2)}$	$\boldsymbol{R}_{(+3)} + 3\boldsymbol{R}_{(+1)} + 3\boldsymbol{R}_{(-1)} + \boldsymbol{R}_{(-3)}$
	$\boldsymbol{R}_{(+1)} - \boldsymbol{R}_{(-1)}$	$\boldsymbol{R}_{(+2)} - \boldsymbol{R}_{(-2)}$	$\boldsymbol{R}_{(+3)} + \boldsymbol{R}_{(+1)} - \boldsymbol{R}_{(-1)} - \boldsymbol{R}_{(-3)}$
2	0	$\boldsymbol{R}_{(+2)} - 2\boldsymbol{R}_{(0)} + \boldsymbol{R}_{(-2)}$	$\boldsymbol{R}_{(+3)} - \boldsymbol{R}_{(+1)} - \boldsymbol{R}_{(-1)} + \boldsymbol{R}_{(-3)}$
3	0	0	$\boldsymbol{R}_{(+3)} - 3\boldsymbol{R}_{(+1)} + 3\boldsymbol{R}_{(-1)} - \boldsymbol{R}_{(-3)}$

Note. The initial product operator states listed in Eq. [39] evolve during irradiation of the I spins in an I_mS_n system according to Eq. [42]. These states are derived from the I-spin polarization with no prior excitation of the S spins. The coefficients $g_\nu^n(\boldsymbol{R})$ of product operators consisting of ν S-spin elements are tabulated in column n as functions of the classical rotation matrices $\boldsymbol{R}_q$ defined in Table 5. The format and usage are similar to Table 3 and the discussion therein. Application of Table 6 to an IS system is provided in Eq. [41]. To use the table for the evolution of the initial states $2I_{xj}S_z$, all $\boldsymbol{R}_0$, $\boldsymbol{R}_{-1}$, and $\boldsymbol{R}_{-3}$ in the table are multiplied by -1 as discussed in the text following Eq. [42].

plying all $\boldsymbol{R}_{(0)}$, $\boldsymbol{R}_{(-1)}$, and $\boldsymbol{R}_{(-3)}$ in Table 6 by -1 which follows from the relation $2P_j^{\pm}S_{j,z} = \pm P_j^{\pm}$ that arises in the derivation.

I_mS_n Systems

For isotropic J-coupling, additional I spins produce no effect other than increasing the initial polarization of I. The subspace propagators $U_{(q)}$ in Eq. [13] become a product composed of individual propagators for each I spin, as in Eq. [28], and the previous rotations become rotations of the total I spin for each component $I_{x_j} = \sum_{i=1}^{m} I_{i,x_j}$. Different scalar couplings J_{IS} merely result in separate rotations of individual I-spin components determined by each $U_{i\,(q)}$.

DISCUSSION

So far, we have presented a theoretical formalism for obtaining the product operator evolution of a weakly coupled I_mS_n system during arbitrary RF irradiation, chosen, without loss of generality, to be applied to the I spins. We then applied this formalism to the initial states of the system that are composed solely of operators for the total I and S spins, since these are the basic states that are generated by pulse sequences employing hard pulses. Exact solutions for the time evolution of the density matrix in terms of its constituent product operator states have been provided in Eqs. [26], [38], and [42].

In the following discussion, we first consider the efficiency of the results for performing simulations. This is followed by a section on spin dynamics, where we illustrate the connection with rotations and the basic simplicity of the solutions, writing them in a form consistent with previous analyses of an IS system (*8, 9*). Further insight into spin dynamics is provided by writing the explicit analytical solutions for the product operator evolution of an IS system during constant on-resonance irradiation of the I spins. We then consider the solutions in the limit where RF field strength is much greater than the coupling strength, which is the relevant domain for many applications. The limit of weak RF fields, which has led to several new applications (*4, 5*), is considered next, followed by a comparison of the exact solutions with those obtained by a frequently used approximation.

Efficiency Issues

The solutions we have obtained for the density operator as a function of time during RF irradiation of the I spins require the C–K parameters $a_q(t_k, t_0)$ and $b_q(t_k, t_0)$ for the simple 2×2 subspaces $U_q(t_k, t_0)$ of the propagator from initial time t_0 to final time $t_k = k\Delta t$. These can be derived from k products of the U_q given in Eq. [13] for each of the constant time intervals of length Δt between t_0 and t_k. The algorithm in Eq. [A3] generates the entire set of C–K parameters labeled by q for the k discrete times in the interval as a sequence of two complex multiplications and one complex addition performed k times. It requires no operations on large matrices, such as diagonalization or matrix multiplication, which are relatively time-consuming procedures of order N^3 for an $N \times N$ matrix, with $N = 2^{n+m}$ for an I_mS_n system of coupled spin-$\frac{1}{2}$ nuclei. In the present method, there are $n + 1$ subspaces with label q ranging from $+n$ to $-n$ in increments $\Delta q = 2$. The equivalent effective fields ω_q defined in Eq. [7] for each subspace completely determine the solutions via the $(n + 1)$ sets of C–K parameters they give rise to. Thus, the computational load scales linearly with the number of spins in an IS_n system rather than as $(2^{n+1})^3$ for a standard density-matrix calculation.

For larger numbers ($m > 1$) of I spins, the solutions merely require additional linear combinations of this basic set of C–K parameters. Moreover, each product operator contribution to the total density operator can be calculated independently of the others. If only the observable signal is of interest, only the S_x component needs to be calculated. In addition, Table 2 shows that each $A_\nu^{(q,r)}$ and $B_\nu^{(q,r)}$ required in Table 4 is the sum of two terms. Results for $\nu = 2, 3$ follow from those for $\nu = 1, 0$, respectively, by changing the sign of the second term, which further improves the efficiency in calculating the full set of solutions. By contrast, the usual matrix-based methods must calculate the full density operator and project it onto the observable component. The other product operator components latent in the density matrix represent unnecessary computational overhead if they are not desired, although the density matrix can be projected onto all possible product operator components for an I_mS_n system by trial and error to determine which components are nonzero, if necessary. In the present method, one knows in advance precisely which operators are generated.

Spin Dynamics

Each U_q for an interval Δt in Eq. [13] is an operator that effects a rotation of an I-spin component I_{x_j} by angle $2\beta_q^k = \omega_q^k \Delta t$ about the axis $\hat{\boldsymbol{\omega}}_q^k$ according to the relation $U_q I_{x_j} U_q^\dagger$. As noted earlier, a classical rotation of this form occurs only for initial states involving no transverse S-spin operators. More

generally, transformations of the form $U_q I_{x_j} U_r^\dagger$ arise (with $r = q - 2$), which have no classical analogue. Successive application of the U_q from time t_0 to time t_k generates the operator $U_q(t_k, t_0)$, which represents an equivalent single rotation $2\varphi_q(t_k)$ about an axis $\hat{\boldsymbol{n}}_q(t_k)$ for each q. The solutions for $\rho_\nu(t_k)$ can be cast in terms of these parameters by inverting the expressions for $a_q(t_k, t_0)$ and $b_q(t_k, t_0)$ analogous to those in Eq. [14] to obtain, at time t_k,

$$\begin{aligned} \varphi_q &= \cos^{-1}[\mathrm{Re}(a_q)] \quad & \hat{n}_{q,z} &= -\mathrm{Im}(a_q)/\sin\varphi_q \\ \hat{n}_{q,x} &= -\mathrm{Re}(b_q)/\sin\varphi_q & \hat{n}_{q,y} &= -\mathrm{Im}(b_q)/\sin\varphi_q. \end{aligned} \qquad [43]$$

This is the form chosen originally in (*8*).[1] Although this approach provides a connection to rotations even when no classical rotations occur, we emphasize that using the C–K parameters directly for simulations is more efficient and is also numerically stable, in contrast to the inversions given in Eq. [43].

The observable signal for each of the initial conditions of Eq. [17] is given in column zero of Table 4 and illustrates the simplicity of the solutions. According to Table 4, the S_x component that evolves during RF irradiation of the I spins in an IS_n system starting with an initial state S_x requires the terms $\Omega_{0,0}^{(q,r)} = \mathrm{Re}\,[A_0^{(q,r)}]$. The particular functions labeled by q and r are given in row 1, column n of Table 3. Using Table 2 and Eq. [A3] for the C–K parameters to calculate $A_0^{(q,r)}$ gives

$$\begin{aligned} \mathrm{Re}[A_0^{(q,r)}] &= \cos\varphi_q \cos\varphi_r + \hat{\boldsymbol{n}}_q \cdot \hat{\boldsymbol{n}}_r \sin\varphi_q \sin\varphi_r \\ &= \frac{1 + \hat{\boldsymbol{n}}_q \cdot \hat{\boldsymbol{n}}_r}{2} \cos(\varphi_q - \varphi_r) \\ &\quad + \frac{1 - \hat{\boldsymbol{n}}_q \cdot \hat{\boldsymbol{n}}_r}{2} \cos(\varphi_q + \varphi_r). \end{aligned} \qquad [44]$$

The observable signal for an initial state $2S_yI_x$ requires $\Omega_{1,0}^{(q,r)}$, which is given by

$$\begin{aligned} \mathrm{Im}[A_1^{(q,r)}] &= -\hat{n}_{q,x} \sin\varphi_q \cos\varphi_r - \hat{n}_{r,x} \cos\varphi_q \sin\varphi_r \\ &\quad - (\hat{n}_{q,y}\,\hat{n}_{r,z} - \hat{n}_{q,z}\,\hat{n}_{r,y}) \sin\varphi_q \sin\varphi_r \\ &= -\tfrac{1}{2}(\hat{\boldsymbol{n}}_q - \hat{\boldsymbol{n}}_r)_x \sin(\varphi_q + \varphi_r) \\ &\quad - \tfrac{1}{2}(\hat{\boldsymbol{n}}_q + \hat{\boldsymbol{n}}_r)_x \sin(\varphi_q - \varphi_r) \\ &\quad - \tfrac{1}{2}(\hat{\boldsymbol{n}}_q \times \hat{\boldsymbol{n}}_r)_x [\cos(\varphi_q - \varphi_r) - \cos(\varphi_q + \varphi_r)]. \end{aligned} \qquad [45]$$

Similar calculations for the initial conditions $2S_yI_y$ and $2S_yI_z$ replace the x component of the rotation axes by the respective y and z components in Eq. [45].

As discussed earlier, q and r are allowed values for the z component of the total S-spin angular momentum (in units of half-integral spin) and satisfy the relation $(q - r)/2 = 1$, which corresponds to the usual selection rule for unit change in the z component. The particular values $q = 1$ and $r = -1$ for an IS system in Eqs. [44] and [45] give, respectively, the solution for the decoupled signal starting with in-phase magnetization S_x (*8*) and the solution for the observable signal starting with two-spin coherence $2S_yI_x$ (*6*).[1] Increasing the number n of S spins in the system increases the number of equivalent effective fields ω_q ($q = +n, \ldots, -n$), which results in a sum of the terms derived from each pair (ω_q, ω_{q-2}), as shown in row 1 of Table 3 and illustrated for a single term of general (q, r) in Eqs. [44] and [45]. For an IS_2 system, the decoupled signal is then $\mathrm{Re}[A_0^{(2,0)}] + \mathrm{Re}[A_0^{(0,-2)}]$, which can be constructed from the general result given in Eq. [44]. For an IS_3 system, it is $\mathrm{Re}[A_0^{(3,1)}] + 2\,\mathrm{Re}[A_0^{(1,-1)}] + \mathrm{Re}[A_0^{(-1,-3)}]$. The number of unique terms multiplying a given product operator component thus increases linearly with the number of S spins, as discussed in the previous section. There are also coefficients of product operator states containing more than one S-spin operator, which are linear combinations of the previously calculated terms, as listed in rows 2 and 3 of Table 3. An illustration for an IS_3 system has already been provided in Eq. [25].

Product operator evolution of IS systems irradiated on resonance. The product operator transformations given in Table 4 are especially simple for the case of constant amplitude, on-resonance irradiation of the I spins in an IS system. In this case, the offset parameter δ in Eq. [1] is equal to zero, so that the effective RF field $\boldsymbol{\omega}_e$ is constant in the transverse plane; the constant equivalent effective fields $\boldsymbol{\omega}_{\pm 1}$ (and unit vectors $\hat{\boldsymbol{\omega}}_{\pm 1} \doteq \hat{\boldsymbol{n}}_{\pm 1}$ associated with them) in each subspace of the propagators $U_{\pm 1}$ have $\pm z$ components given by Eq. [7], and the rotation angles $\beta_{\pm 1} \doteq \varphi_{\pm 1}$ derived from Eq. [12] increase linearly with time. For RF phase $\phi = 0$ in Eq. [1], we have

$$\omega_{\pm 1} = [(\omega_{\mathrm{rf}})^2 + (\mathcal{J}/2)^2]^{1/2} \doteq \omega_e^{\mathcal{J}} \qquad [46]$$

$$\varphi_{\pm 1} = \tfrac{1}{2}\omega_e^{\mathcal{J}} t \doteq \varphi \qquad [47]$$

$$(\hat{n}_{\pm 1})_x = \omega_{\mathrm{rf}}/\omega_e^{\mathcal{J}} \doteq \hat{n}_x \qquad [48]$$

$$(\hat{n}_{\pm 1})_z = \pm\frac{\mathcal{J}/2}{\omega_e^{\mathcal{J}}} \doteq \pm\hat{n}_z \qquad [49]$$

to give

$$\begin{aligned} a_{\pm 1} &= \cos\varphi \mp i\hat{n}_z \sin\varphi \\ b_{\pm 1} &= -i\hat{n}_x \sin\varphi \end{aligned} \qquad [50]$$

from Eq. [14]. The necessary products of these C–K parameters are given in Table 2 for the required coefficients of the various states in Table 4. The evolution of each initial state

[1] The rotation convention and angles defined in Refs. (*6*) and (*8*) correspond to transforming φ in the present work to $-\varphi/2$.

denoted by the index ν in Eq. [17] is given by the corresponding row in Table 4. Using the relation $\hat{n}_x^2 + \hat{n}_z^2 = 1$ and the trigonometric half-angle relations to write both $\sin^2(\varphi)$ and $\cos^2(\varphi)$ in terms of $\cos(2\varphi)$, we obtain

$$S_x \rightarrow (\hat{n}_x^2 + \hat{n}_z^2 \cos 2\varphi)S_x - \hat{n}_x\hat{n}_z(1 - \cos 2\varphi)2S_yI_y + \hat{n}_z \sin(2\varphi)2S_yI_z \quad [51]$$

$$2S_yI_x \rightarrow 2S_yI_x \quad [52]$$

$$2S_yI_y \rightarrow -\hat{n}_x\hat{n}_z(1 - \cos 2\varphi)S_x + (\hat{n}_z^2 + \hat{n}_x^2 \cos 2\varphi)2S_yI_y + \hat{n}_x \sin(2\varphi)2S_yI_z \quad [53]$$

$$2S_yI_z \rightarrow -\hat{n}_z \sin(2\varphi)S_x - \hat{n}_x \sin(2\varphi)2S_yI_y + \cos(2\varphi)2S_yI_z \quad [54]$$

for the time evolution of the product operator states during on-resonance RF irradiation of the I spins in an IS system. The explicit dependence of these transformations on the applied RF field and the coupling are obtained from the substitutions in Eqs. [46–49].

The transformations of the initial states of Eq. [39], containing no transverse S-spin operators, are obtained similarly using Table 5 to construct the 3D rotation matrices $\boldsymbol{R}_{\pm 1}$ utilized in the example of Eq. [41], which is the application of Table 6 to a simple IS system. As noted in the discussion following Eq. [42], the transformations of the initial states $2I_{x_j}S_z$ are also obtained from Eq. [41] by making the substitution $\boldsymbol{R}_{-1} \rightarrow -\boldsymbol{R}_{-1}$. In other words, I_{x_j} and $2I_{x_j}S_z$ are interchanged in Eq. [41]. For on-resonance irradiation and RF phase equal to zero, the same parameters in Eqs. [46–49] can be identified in Table 5, where $\sin\theta_{\pm 1} = \hat{n}_x$, $\cos\theta_{\pm 1} = \pm\hat{n}_z$, and $\beta_{\pm 1} = \varphi$. The rotations are applied only to the I-spin operators, and each I_{x_j} is represented as the usual unit vector with element j equal to 1 and the other elements equal to zero. Thus, for example, operator I_x picks out the first column of $\boldsymbol{R}_{\pm 1}$ with the elements in each row giving the coefficients of I_x, I_y, and I_z. The required addition and subtraction of $\boldsymbol{R}_{\pm 1}I_{x_j}$ in Eq. [41] gives

$$I_x \rightarrow (\hat{n}_x^2 + \hat{n}_z^2 \cos 2\varphi)I_x + \hat{n}_z \sin(2\varphi)2I_yS_z + \hat{n}_x\hat{n}_z(1 - \cos 2\varphi)2I_zS_z \quad [55]$$

$$I_y \rightarrow \cos(2\varphi)I_y + \hat{n}_x \sin(2\varphi)I_z - \hat{n}_z \sin(2\varphi)2I_xS_z \quad [56]$$

$$I_z \rightarrow -\hat{n}_x \sin(2\varphi)I_y + (\hat{n}_z^2 + \hat{n}_x^2\cos 2\varphi)I_z + \hat{n}_x\hat{n}_z(1 - \cos 2\varphi)2I_xS_z \quad [57]$$

$$2I_xS_z \rightarrow (\hat{n}_x^2 + \hat{n}_z^2 \cos 2\varphi)2I_xS_z + \hat{n}_z \sin(2\varphi)I_y + \hat{n}_x\hat{n}_z(1 - \cos 2\varphi)I_z \quad [58]$$

$$2I_yS_z \rightarrow \cos(2\varphi)2I_yS_z + \hat{n}_x \sin(2\varphi)2I_zS_z - \hat{n}_z \sin(2\varphi)I_x \quad [59]$$

$$2I_zS_z \rightarrow -\hat{n}_x \sin(2\varphi)2I_yS_z + (\hat{n}_z^2 + \hat{n}_x^2 \cos 2\varphi)2I_zS_z + \hat{n}_x\hat{n}_z(1 - \cos 2\varphi)I_x. \quad [60]$$

Results analogous to Eqs. [51–60] are obtained for an IS_n system by appropriate modification of the parameters in Eqs. [46–50], as described in the previous section. We next consider the general product operator solutions for the evolution of the density matrix, as well as the particular solutions above, in the limits of both strong and weak RF fields.

Strong RF Fields ($\boldsymbol{\omega}_e \gg \mathcal{J}$)

During an adiabatic inversion pulse, the vector model of decoupling (*3*) would predict very simply that the observable S-spin signal $f_1^n(\Omega_{\nu 0})$ is independent of n in an IS_n system, except for a larger signal as the number of S spins in the system increases. Since the evolution of the S spins in the model depends only on the orientation of a semiclassical I-spin vector, and there is only a single I operator in the system, the I–S interaction is the same for all n. The same, but more general, conclusion was reached in (*11*) for the coefficients of $2S_yI_{x_j}$ generated during adiabatic decoupling, based on the results of simulations. However, the equality of the solutions for different n is not limited to adiabatic pulses, and the present solutions show explicitly why this is so for any RF pulse of sufficiently large amplitude.

Under the condition $\omega_e \gg \mathcal{J}$, differences among the ω_q that determine the solution for $\rho(t)$ are relatively insignificant. As an illustration to provide a sense of scale, a coupling of 150 Hz and a simple on-resonance pulse of constant amplitude 3 kHz gives $\omega_q/(2\pi)$ equal to 3.001, 3.004, and 3.008 kHz for $q = 1$, 2, and 3, respectively. There is thus a variation of only a few tenths of a percent among the different ω_q, and all the $\Omega^{(q,r)}$ of Table 3 are equal to the extent that the effective applied RF field is sufficiently large. As a result, the coefficients f_i^n for $i >$ 1 in Table 3, corresponding to terms in Eq. [26] with more than one S-spin operator, are zero in the limit of large RF. This simple equivalence of the solutions for all IS_n breaks down when the RF field becomes small enough that different ω_q produced by the coupling among the RF field, I, and S produce significant effects. In the example above, a smaller RF amplitude of 1 kHz gives variations on the order of a percent for $\omega_q/(2\pi)$ equal to 1.003, 1.011, and 1.025 kHz, and differences in the solutions for increasing numbers of S spins become more apparent.

For the on-resonance solutions of Eqs. [51–60], if $\omega_{rf} \gg \mathcal{J}$ then $\hat{n}_x \approx 1$, $\hat{n}_z \approx 0$, and there are no surprises. The I-spin operators in Eqs. [55–60] precess about the RF field according to expectation for a standard hard pulse on the I spins. In Eqs. [51–54], the observable signal is proportional to the S_x component. Initial in-phase magnetization S_x in Eq. [51] produces upon Fourier transformation a large, constant (DC) component proportional to $\hat{n}_x^2$ (i.e., it is decoupled) with small sidebands of

relative amplitude $\hat{n}_z^2/2$ due to the $\cos(2\varphi) \approx \cos(\omega_{rf}t)$ oscillation imposed on the signal (*8, 13*). In addition, the interconversion of $2S_yI_y$ and $2S_yI_z$ given in Eqs. [53] and [54] results in well-known phase anomalies from initial two-spin coherence or antiphase magnetization if the signal is acquired after the RF has been turned off (*12*). There is no observable signal in these cases for acquisition with the decoupler on, since the S_x component depends on $\hat{n}_z$ and is thus vanishingly small.

However, there are interesting new effects that are evident in the exact solutions of Eqs. [51–60] when the RF field strength is on the order of the coupling, so that $\hat{n}_z$ is of appreciable magnitude. These are considered in the next section together with a comparison of the general solutions with previously obtained results.

Weak RF Fields ($\boldsymbol{\omega}_e \approx \mathcal{J}$)

As discussed in the previous section, the solutions are different for different numbers of S spins in the weak-field case, which is well known from continuous-wave (CW) decoupling using RF of constant amplitude and phase. Exact solutions for the observable signal during CW irradiation starting with in-phase magnetization in an I_mS_n system are listed in Tables I–III of Ref. (*13*) (the roles of I and S are interchanged compared to the usage here). In the present work, both the amplitude and the frequency of the observed S-spin signal can be readily obtained from Eq. [44]. For constant RF, $\varphi_q = \frac{1}{2}\omega_q t$ and $\hat{\boldsymbol{n}}_q \cdot \hat{\boldsymbol{n}}_r \doteq \hat{\boldsymbol{\omega}}_q \cdot \hat{\boldsymbol{\omega}}_r = \cos(\theta_q - \theta_r)$, with ω_q and θ_q defined in Eq. [7] and Eq. [8], respectively, which facilitates the comparison with the results in Ref. (*13*). For IS_n, the allowed values for q and r appear as the superscripts in the first row of Table 3, which gives the sum of terms constructed from $\mathrm{Re}[A_0^{(q,r)}]$ that comprise the solution for the signal. For I_mS, we have $q = 1$, $r = -1$, and the observed signal is given by Eq. [44] raised to the power m, as noted in the discussion following Eq. [33].

As an example, if we observe the S spin in an I_3S system during irradiation of the I spins, then in the limit $\omega_{rf} \rightarrow 0$, the solutions must yield lines at $\pm J/2$ and $\pm 3J/2$ in the ratio 1:3:3:1. Cubing Eq. [44] and performing the necessary trigonometric rearrangements to obtain simple (raised to the first power) cosine functions of the angles $\varphi_{\pm 1}$ for the time dependence of the signal gives eight terms that lead to the eight pairs of $\pm$frequencies in Table III upon Fourier transformation of the signal. Of these eight cosine terms, we consider only the two that have nonzero amplitude when the RF is turned off. Defining α as the angle between $\hat{\boldsymbol{n}}_{+1} \doteq \hat{\boldsymbol{\omega}}_{+1}$ and $\hat{\boldsymbol{n}}_{-1} \doteq \hat{\boldsymbol{\omega}}_{-1}$ gives $\hat{\boldsymbol{n}}_{+1} \cdot \hat{\boldsymbol{n}}_{-1} = \cos\alpha$, and we obtain

$$S_x \sim \tfrac{3}{8}(1 - \cos\alpha)[3(1 + \cos^2\alpha) + 2\cos\alpha] \times \cos(\varphi_{+1} + \varphi_{-1}) + \tfrac{1}{8}(1 - \cos\alpha)^3 \times \cos 3(\varphi_{+1} + \varphi_{-1}) + \{\text{terms} \rightarrow 0 \text{ as } \omega_{rf} \rightarrow 0\}. \quad [61]$$

Then, for $\omega_{rf} = 0$, we have $\boldsymbol{\omega}_{\pm 1} = \pm\mathcal{J}/2\,\hat{\mathbf{z}}$, $\varphi_{\pm 1} = \mathcal{J}t/4$ from Eqs. [46] and [47], $\alpha = \pi$ so that

$$S_x \rightarrow 3\cos\tfrac{1}{2}\mathcal{J}t + \cos\tfrac{3}{2}\mathcal{J}t \quad [62]$$

as required. In Tables I–III (*13*), $A(m)$ and $\varphi(m)$ correspond to ω_{2m} and α, respectively, in the present work. There is an apparent typesetting error in the expression for the line intensity in rows 6 and 9 of Table III, which corresponds to the first term in Eq. [61] above. For $\omega_{rf} = 0$, so there is only the coupling interaction, Table III as written yields a quartet with equal line intensities. We also obtain $\frac{3}{8}(1 + \cos\alpha)[3(1 + \cos^2\alpha) - 2\cos\alpha]$ for the amplitude of the $\cos(\varphi_{+1} - \varphi_{-1})$ term not shown in Eq. [61], which corresponds to rows 2 and 3 in Table III. For an I_2S system, we take the square of Eq. [44] and find a constant, DC term of amplitude $\frac{1}{2}(1 + \cos^2\alpha)$ relative to the expression $\cos^2\alpha$ for the corresponding term in row 2 of Table II. Both of these expressions give the correct unit amplitude for this frequency component when $\omega_{rf} = 0$ ($\alpha = \pi$), but the current solutions accurately predict a minimum value of $\frac{1}{2}$ for the intensity when $\alpha = \pi/2$, i.e., $\omega_{rf} = \mathcal{J}/2$, so the centerband S-spin signal in an I_2S system never vanishes.

The complete solutions for the density operator obtained here reveal a number of interesting new phenomena at low RF field strength. In Eq. [53], the observable S_x magnetization that evolves from the initial $2S_yI_y$ state has a DC component proportional to $\hat{n}_x\hat{n}_z$, with a maximum value equal to $\frac{1}{2}$ when $\omega_{rf} = \mathcal{J}/2$, that mimics the signal from in-phase magnetization in Eq. [51]. Sidebands of relative amplitude $\hat{n}_x\hat{n}_z/2$ appear at $\pm\omega_e^{\mathcal{J}}$ due to the $\cos(2\varphi) = \cos(\omega_e^{\mathcal{J}}t)$ term. The frequency spectrum of the sidebands depends sensitively on RF field homogeneity, according to Eq. [46]. These issues and others are discussed more fully in Ref. (*4*), where novel methods are provided for characterizing a decoupler channel for the insensitive spins by observing large signals with the sensitive-spin channel.

For the case $\omega_{rf} = \mathcal{J}/2$, so that $\hat{n}_x = \hat{n}_z = 1/\sqrt{2}$, the simplified transformations that can be derived from Eqs. [51–54] were obtained independently by experiment prior to the general quantum mechanical solutions, using a vector picture of the relevant spin states. The product operator transformations therefore provide the basis for a literal vector interpretation of spin evolution during RF irradiation. This model, which has proven useful in envisioning new sequences and applications, will be detailed in a subsequent publication. For now, we merely note that for $\omega_{rf} = \mathcal{J}/2$, Eqs. [51] and [53] show that the interconversions $S_x \rightleftarrows 2S_yI_y$ occur in 100% yield for $\varphi = \pi/2$, i.e., at time $t = (\sqrt{2}J)^{-1}$. Further analysis shows that the effects have a sensitive dependence on resonance offset, and analogous results are evident in Eqs. [55–60] for the evolution of states derived from the I-spin polarization. Applications for these new selective coherence transfer pulses are discussed in detail in Ref. (*5*).

In the limit where the RF field is zero, we have $n_x = 0$, $n_z =$

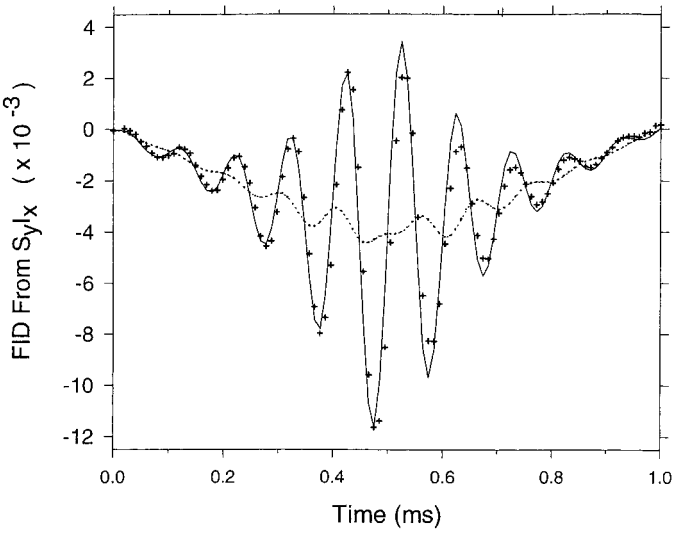

FIG. 1. The signal resulting from $2S_yI_x$ at the start of a decoupled acquisition is plotted as a function of time during a sech/tanh adiabatic inversion pulse of x phase applied to the I spins of an IS system ($^{13}CH_3I$). Further details can be found in Ref. (*3*). Predictions of the tilted frame approximation (dotted line), as discussed in the text, are compared with the exact solutions provided here (solid line) and experiment (+). A constant magnitude decoupling field of 10 kHz was employed, which is almost two orders of magnitude larger than the coupling, $J = 150$ Hz, illustrating that the tilted frame approximation may not be sufficiently precise, even when the condition $\omega_e \gg \mathcal{J}$ is fulfilled.

1, and $\varphi = \mathcal{J}/4$ in Eqs. [51–54] to obtain the standard product operator rules for coupling evolution of an IS system.

Comparison with Tilted Frame Methods

We refer to tilted frame methods as those which transform the Hamiltonian to a frame in which the instantaneous direction of the effective field (*11*) or fields, in the case of double resonance (*14, 15*), defines the z axis. The large off-diagonal RF terms in the usual rotating-frame Hamiltonian are transformed to diagonal elements in the tilted frame. Small off-diagonal elements in the tilted frame are of magnitude $\mathcal{J}/\omega_e$ relative to the diagonal elements and are typically discarded to diagonalize $\mathcal{H}$ in this approximation. The original problem is then easily solved in the tilted frame and transformed back to the rotating frame, with the effect of the omitted terms expected to be negligible in the limit $\omega_e \gg \mathcal{J}$. Applications include solutions for adiabatic decoupling (*11*) and cross polarization/double resonance (*14, 15*). The question left open is When do the terms that were set equal to zero become important? Since the approximate solution ignores their effect altogether, there is no reliable measure in this method for quantifying the accuracy of the solution, and trial-and-error comparisons with exact simulations cannot cover all possibilities. Furthermore, one is not assured that the approximation is sufficiently accurate unless the exact answer is known.

Figure 1 shows the experimental and theoretical S-spin signal during a sech/tanh inversion pulse of x phase applied to the I spins of an initial $2S_yI_x$ configuration, with $J_{CH} = 150$ Hz (*3*). Predictions of the tilted-frame solution (*11*) are overlayed for comparison. Although the constant-magnitude effective field of 10 kHz used for the sech/tanh waveform in this example is almost two orders of magnitude larger than the coupling, so that $\omega_e \gg \mathcal{J}$, the time-dependent amplitude of the actual signal, and therefore the sidebands in the Fourier-transformed spectrum, are an order of magnitude larger than what is predicted by the approximation. An increasingly widespread disagreement between the exact and approximate solutions for more general initial conditions occurs at the lower power levels used in practice to reduce sample heating and produce the most efficient adiabatic decoupling, even though the condition $\omega_e \gg \mathcal{J}$ is still satisfied. We have shown previously that the intensity of cycling sidebands from in-phase magnetization is a useful standard for the efficiency of adiabatic decoupling sequences (*16, 17*). The exact solutions were instrumental in determining decoupling parameters that provide optimal performance under practical experimental conditions.

We observe, also, that the tilted frame prediction for the signal from coherences of the form $2S_yI_{x_j}$ during simple on-resonance CW decoupling is identically zero for RF of any amplitude, which would support the longstanding, but erroneous, perception that these states produce no useful signal during RF irradiation of one of the spins. By contrast, the exact solutions, which produce reliable results for any RF waveform, recently inspired several novel applications (*4, 5*) for weak-field RF. An issue that remains open is the precision of the tilted frame approach for double resonance of the I and S spins, but this is a more computationally intensive problem that is beyond the scope of the present article.

CONCLUSION

The dynamics of weakly coupled I_mS_n systems during arbitrary RF irradiation of the I spins have been considered. Exact solutions for the time evolution of the density matrix in terms of its constituent product operator states have been obtained for any initial state that is composed solely of operators for the total I and S spins. Solutions for other initial conditions can be obtained similarly. We began by deriving the general solution for IS_n systems in Eq. [26]. The coefficients of the various product operator terms in the solution are simple functions, defined in Table 3, of the arguments listed in Table 4. To clarify the structure of the general solution, the evolution of an IS_3 system initially in the state S_x is provided in expanded form in Eq. [25]. The solutions for I_mS_n systems in Eq. [38] (initial states derived from S-spin polarization) and Eq. [42] (initial states derived from I-spin polarization) are simple extensions of this basic form.

If the amplitude and phase of the RF irradiation are constant, the solutions reduce to straightforward analytical expressions that predict several interesting effects due to the coupling among I, S, and the RF field. The product operator rules for the evolution of

IS systems during constant, on-resonance RF irradiation of the I spins are provided in Eqs. [51–60]. A brief overview of applications derived from these predictions has been presented. Solutions for the signals that occur during irradiation of coherences of the form $2S_yI_{xj}$, together with methods for eliminating them, have been published previously (*6*), and the time development of an IS spin system during a weak amplitude square pulse (as in continuous-wave decoupling) has yielded novel characterization-of-decoupler (COD) sequences for calibrating an insensitive I-spin channel by observing large signals from these same coherences with the S-spin channel (*4*). Applications for selective NMR of large molecules using new "*J*-pulses" derived from the solutions have also been proposed (*5*). The full details of those calculations can be found here. The time to compute a given product operator component (i.e., the number of floating point operations) for a general RF waveform delivered in a series of fixed increments scales linearly with the number of spins, N, in the system. By comparison, the computation time of simulations which require matrix diagonalization or multiplication of large matrices is of order $(2^N)^3$. Additional efficiencies are noted in the correspondingly entitled section of the Discussion. We also showed that results obtained using a tilted frame approximation may not be sufficiently precise, even though the condition $\omega_e \gg \mathcal{J}$ employed in its derivation is satisfied.

We close by mentioning several areas for future research. The exact product operator evolution of the density matrix during RF irradiation of one nuclear species provides a detailed physical picture of *J*-coupling modulation during RF pulses that has not been available previously, and this will be described at a later date. The Cartesian product operator basis employed here is easily transformed to any alternate basis that might prove advantageous in analyzing an experiment (see, for example, (*18*) and references therein), so that the present results can be extended to include analysis of coherence pathways (*19*, *20*) generated by completely general RF waveforms. Since the formalism presented here is equally valid in the absence of either RF irradiation or the coupling, the solutions encompass any combination of arbitrary RF waveforms, delays, and coherence gradients to provide a general method for efficient pulse sequence simulation.

APPENDIX

Algorithm for Generating the Cayley–Klein Parameters

The evolution of the density operator from an initial time t_0 to a final time t_k is determined by the time-evolution operator $U(t_k, t_0)$, which is composed of the individual rotation operators $U_q(t_k, t_0)$ in each subspace according to Eq. [15]. The solution for the density operator has been compiled in Tables 2–4 in terms of the C–K parameters $a_q(t_k)$ and $b_q(t_k)$. These parameters are obtained by successive application of the rotation operators $U_q(t_k, t_{k-1})$ defined in Eq. [13] for each of the k intervals of length Δt between the initial and final times, as derived from the time-independent Hamiltonian for each interval. For each matrix multiplication, only the two first-row elements of the product matrix need to be computed, since the other two elements can be obtained by complex conjugation. An efficient algorithm starts with

$$a_q(t_1) = a_q^1, \quad b_q(t_1) = b_q^1, \tag{A1}$$

as defined in Eq. [14] for each a_q^k and b_q^k during the kth interval $t_k - t_{k-1}$. For $k > 2$, the matrix products

$$U_q(t_k, t_{k-1})U_q(t_{k-1}, t_0) = \begin{pmatrix} a_q^k & b_q^k \\ -b_q^{k*} & a_q^{k*} \end{pmatrix} \times \begin{pmatrix} a_q(t_{k-1}) & b_q(t_{k-1}) \\ -b_q^*(t_{k-1}) & a_q^*(t_{k-1}) \end{pmatrix} \tag{A2}$$

then give

$$\begin{aligned} a_q(t_k) &= a_q^k\, a_q(t_{k-1}) - b_q^k\, b_q^*(t_{k-1}) \\ &= \cos\varphi_q - i\hat{n}_{q,z}\sin\varphi_q \\ b_q(t_k) &= a_q^k\, b_q(t_{k-1}) + b_q^k\, a_q^*(t_{k-1}) \\ &= -(\hat{n}_{q,y} + i\hat{n}_{q,x})\sin\varphi_q \end{aligned} \tag{A3}$$

for the rotation operator $U_q(t_k, t_0)$ in terms of the equivalent single rotation $2\varphi_q(t_k)$ about the axis $\hat{\boldsymbol{n}}_q(t_k)$ for each q, as defined in Eq. [43].

Expansion Coefficients $\alpha_{\nu\mu}^{(q,r)}$ in Eq. [24]

The solution for the density matrix in terms of its constituent product operator states was obtained by expanding the products $U_q 2I_{x_\nu} U_r^\dagger$ ($\nu = 0, \ldots, 3$) as linear combinations of the I-spin operators

$$\begin{aligned} 2I_{x_0} &= \begin{pmatrix} 1 & 0 \\ 0 & 1 \end{pmatrix} \quad 2I_x = \begin{pmatrix} 0 & 1 \\ 1 & 0 \end{pmatrix} \\ 2I_y &= \begin{pmatrix} 0 & -i \\ i & 0 \end{pmatrix} \quad 2I_z = \begin{pmatrix} 1 & 0 \\ 0 & -1 \end{pmatrix} \end{aligned} \tag{A4}$$

in the standard matrix representation. Using Eq. [13] or Eq. [A2] for the matrix representation of the rotation operator U_q in the subspace, denoted by q, of the total propagator produces results of the form

$$\begin{aligned} U_q 2I_{x_0} U_r^\dagger &= \begin{pmatrix} A_0 & B_0 \\ -B_0^* & A_0^* \end{pmatrix} \quad U_q 2I_x U_r^\dagger = \begin{pmatrix} A_1 & B_1 \\ B_1^* & -A_1^* \end{pmatrix} \\ U_q 2I_y U_r^\dagger &= -i\begin{pmatrix} A_2 & B_2 \\ -B_2^* & A_2^* \end{pmatrix} \quad U_q 2I_z U_r^\dagger = \begin{pmatrix} A_3 & B_3 \\ B_3^* & -A_3^* \end{pmatrix}, \end{aligned} \tag{A5}$$

with the elements A_ν and B_ν listed in Table 2 in terms of the

appropriate Cayley–Klein parameters and indices (q, r). An arbitrary 2×2 matrix

$$M = \begin{pmatrix} A & B \\ C & D \end{pmatrix} \qquad [A6]$$

can be expanded as

$$\begin{aligned} M &= A(I_{x_0} + I_z) + B(I_x + iI_y) + C(I_x - iI_y) + D(I_{x_0} - I_z) \\ &= (A + D)I_{x_0} + (B + C)I_x + i(B - C)I_y + (A - D)I_z. \end{aligned} \qquad [A7]$$

For the matrices of Eq. [A5], we write $w + w^* = 2\,\mathrm{Re}(w)$ and $w - w^* = 2i\,\mathrm{Im}(w)$ for complex w to obtain the expressions listed in Table 1. Alternatively, M can be expanded in terms of any other suitable basis, resulting in corresponding modifications to the elements in Table 1.

REFERENCES

1. O. W. Sørensen, G. W. Eich, M. L. Levitt, G. Bodenhausen, and R. R. Ernst, Product operator formalism for the description of NMR pulse experiments, *Prog. NMR Spectrosc.* **16,** 163–192 (1983).
2. R. J. M. Van den Ven and C. W. Hilbers, A simple formalism for the description of multiple-pulse experiments. Application to a weakly coupled two-spin ($I = \frac{1}{2}$) system, *J. Magn. Reson.* **54,** 512–520 (1983).
3. T. E. Skinner and M. R. Bendall, A vector model of adiabatic decoupling, *J. Magn. Reson.* **134,** 315–330 (1998).
4. M. R. Bendall and T. E. Skinner, Novel methods for characterizing a decoupler channel using "undetectable" quantum coherences, *J. Magn. Reson.* **139,** 175–180 (1999).
5. M. R. Bendall and T. E. Skinner, *J* pulses for multiplet-selective NMR, *J. Magn. Reson.* **141,** 261–270 (1999).
6. M. R. Bendall and T. E. Skinner, Coherence sidebands in adiabatic decoupling, *J. Magn. Reson.* **129,** 30–34 (1997).
7. R. Bazzo and J. Boyd, Pulse shaping and selective excitation. The effect of scalar coupling, *J. Magn. Reson.* **79,** 568–576 (1988).
8. J. S. Waugh, Theory of broadband spin decoupling, *J. Magn. Reson.* **50,** 30–49 (1982).
9. A. J. Shaka and J. Keeler, Broadband spin decoupling in isotropic liquids, *Prog. NMR Spectrosc.* **19,** 47–129 (1987).
10. A. J. Shaka, Composite pulses for ultra-broadband spin inversion, *Chem. Phys. Lett.* **120,** 201–205 (1985).
11. C. Zwahlen, S. J. F. Vincent, and L. E. Kay, Analytical description of the effect of adiabatic pulses on IS, I_2S, and I_3S spin systems, *J. Magn. Reson.* **130,** 169–175 (1998).
12. M. H. Levitt, G. Bodenhausen, and R. R. Ernst, The illusions of spin decoupling, *J. Magn. Reson.* **53,** 443–461 (1983).
13. W. A. Anderson and R. Freeman, Influence of a second radiofrequency field on high-resolution nuclear magnetic resonance spectra, *J. Chem. Phys.* **37,** 85–103 (1962).
14. L. Müller and R. R. Ernst, Coherence transfer in the rotating frame. Application to heteronuclear cross-correlation spectroscopy, *Mol. Phys.* **38,** 963–992 (1979).
15. D. E. Demco, H. Köstler, and R. Kimmich, Adiabatic *J* cross polarization with and without localization, *J. Magn. Reson. A* **110,** 136–145 (1994).
16. T. E. Skinner and M. R. Bendall, Peak power and efficiency in hyperbolic-secant decoupling, *J. Magn. Reson. A* **123,** 111–115 (1996).
17. M. R. Bendall and T. E. Skinner, Calibration of STUD+ parameters to achieve optimally efficient broadband adiabatic decoupling in a single transient, *J. Magn. Reson.* **134,** 331–349 (1998).
18. A. Bain, The superspin formalism for pulse NMR, *Prog. NMR Spectrosc.* **20,** 295–315 (1988).
19. A. Bain, Coherence levels and coherence pathways in NMR. A simple way to design phase cycling procedures, *J. Magn. Reson.* **56,** 418–427 (1984).
20. G. Bodenhausen, H. Kogler, and R. R. Ernst, Selection of coherence-transfer pathways in NMR pulse experiments, *J. Magn. Reson.* **58,** 370–388 (1984).